DEFORMATION MONITORING AND TIME-SERIES & DISASTER POTENTIALITY ANALYSIS OF GAS PIPELINE USING SENTINEL DATA

Xiaoqing Wang[1], Peng Zhang[1], Junli Wu[1*], Zhicai Li[2], Wei Tang[2], Zhanyi Sun[1]

[1] National Geomatics Center of China, Beijng, China-(xqwang, pzhang, jlwu, szy) @ngcc.cn
[2] China University of Mining and Technology-Beijing, Beijing, China-(24806605, 351212085) @qq.com

KEY WORDS: deformation, time-series, disaster, gas pipeline, sentinel.

ABSTRACT:

Synthetic aperture radar interferometry (InSAR) measurement technology is a new remote sensing technology that can effectively monitor slight land deformation. Compared with traditional monitoring technology, InSAR technology has the advantages of wide coverage, all-weather and low cost, providing a technical means of high-resolution, high-precision and low-cost for hidden geological hazard identification and deformation monitoring along pipelines. For purpose of this paper, we performed deformation time-series comprehensive processing and analysis on gas pipeline based on Sentinel-1 image data through small baseline data processing, and extracted pipeline deformation quantities from 2020 to 2022. The land deformation rate of the ascending track data during this period ranges from -43 mm/year to 25 mm/year, and that of the descending track data from -66 mm/year to 33 mm/year. The results show that the area along the gas pipeline is in stable condition on the whole, deformation mainly occurred along a section in the northwest of Haidian District, and a large quantity of deformation occurred since January of 2020 until December of 2021, with the maximum deformation quantity of -70mm, This result provided a reliable reference for safety monitoring and repair & maintenance of the gas pipeline.

1. INTRODUCTION

Synthetic aperture radar interferometry (InSAR) measurement technology is a new remote sensing technology that can effectively monitor slight land deformation (Wang Xiaoqing et al,2018). Compared with traditional monitoring technology, InSAR technology has the advantages of wide coverage, all-weather and low cost, and it has been applied to urban land subsidence monitoring. Foreign scholars Ferretti et al. proposed time-series analysis techniques such as PS-InSAR and SBAS-InSAR to improve the reliability of deformation monitoring (GAO Ertao et al,2019). SBAS-InSAR technology selects images with short time baselines in multiple images acquired and combines them into several small sets, conducting deformation monitoring even with a small number of images. Furthermore, it can greatly reduce the de-coherence between interfering images and take all coherent point information into account when remove the atmospheric phase, leading to better atmospheric phase removal effect.

Business Synthetic Aperture Radar Interferometry (InSAR) provides a technical means of high-resolution, high-precision and low-cost for hidden geological hazard identification and deformation monitoring along pipelines. Based on time series of phase information, InSAR technology enables identifying slight deformation in a large area. Thus, this technology is largely superior for detection of disasters and hidden troubles caused by deformation in a large area. InSAR technology has been widely applied for landslide danger detection and identification in the Three Gorges Area, Jinsha River Watershed, southwestern mountainous area, area along Sichuan-Tibet Railway, and Loess Plateau, and a large number of research achievements have been obtained. Small Baseline Subset Interferometry (SBAS-InSAR) is a new time-series analysis method for slight land deformation monitoring proposed by P.Berardino et al. in 2002. This technology can overcome the limiting factors (temporal and perpendicular de-coherence, effect of atmospheric conditions, etc.) that Differential Interferometric Synthetic Aperture Radar (D-InSAR) is subject to during data processing, so that it can be used to monitor slight land deformation continuously at millimeter-level precision. For purpose of this paper, we employed small baseline set synthetic aperture radar interferometry technology to perform time-series interferometric processing on Sentinel-1 image data of Liangxi section of Shanxi-Beijing Third Line, combined ascending track method with descending track method to extract the annual average land deformation rate distribution map of this area from January 5 of 2020 to October 9 of 2022 to figure out the average ascending track and descending track deformation rates of the area, and explored the causes of deformation based on the geologic characteristics and infrastructure construction in this area.

2. RESEARCH AREA AND DATA

2.1 Research Area

Liangxi section is mainly located in the west of Beijing, traveling through Fangshan District, Fengtai District, Mentougou District, Haidian District, and Changping District. It is currently the longest urban pipeline with the largest diameter around China. Various terrains are distributed along the pipeline, where the topography and geologic environment are complex, and there exists a danger of various geological hazards such as landslide, collapse, debris flow, mining collapse, etc. Thus, detecting geological hazards along the pipeline is greatly important to the design, construction and safe operation of pipeline project. Figure 1 shows coverage of Sentinel-1 ascending track data of the section in western Beijing, and Figure 2 shows coverage of Sentinel-1 descending track data of the section in western Beijing.

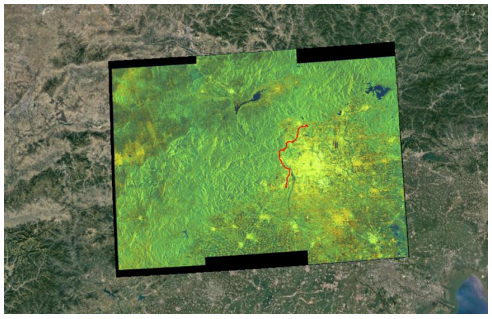

Figure 1. Coverage of Sentinel-1 ascending track data. Red line indicates the pipeline

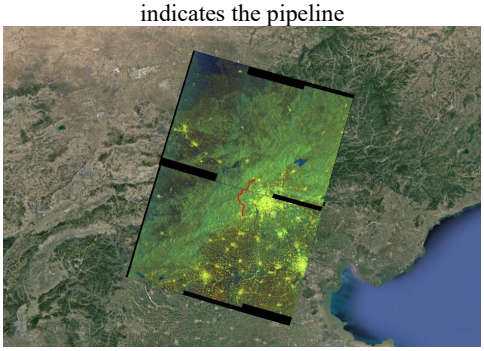

Figure 2 Coverage of Sentinel-1 descending track data. Red line indicates the pipeline

2.2 Experimental Data

Sentinel-1 satellite is an earth observation satellite launched by European Space Agency for the Copernicus Initiative. It is a two-constellation satellite that is able to provide continuous monitoring image for 24 hours, carries perfect polarization right view C-band synthetic aperture radar at the band frequency of 5.405GHz, and has a revisit interval of 12 days. Its advanced radar system can penetrate through clouds to perform all-time all-whether earth observation and track changes of land-use patterns and ground settlement, which is significant for practical use.

For purpose of this paper, the following materials and parameters are adopted: Sentinel-1 interferometric wide image of the European Space Agency; C-band (wavelength 5.6cm) with resolution of 5×20m; IW model data; width of 250km. Sentinel-1 is a two-constellation satellite. A single Sentinel-1 constellation covers the whole world once every 12 days, so two constellations can shorten the revisit interval to 6 days. In this research, the Sentinel-1 data covering 117 scenes in the research area (84 ascending track + 33 descending track) from January 5 of 2020 to October 9 of 2022 was adopted. Table 1 shows ascending track data, and Table 2 shows descending track data. According to the operating principle of the abovementioned SBAS-InSAR technology, the temporal baseline threshold of interferometric image combination was set as 50 days, and the perpendicular baseline threshold as 100 meters. 254 pairs of interferometric image had been developed for the ascending track, and 81 pairs for the descending track.

Date	Track Direction	Date	Track Direction
20200105	Ascending	20200117	Ascending
20200129	Ascending	20200210	Ascending
20200222	Ascending	20200305	Ascending
20200317	Ascending	20200329	Ascending
20200410	Ascending	20200422	Ascending
20200504	Ascending	20200516	Ascending
20200528	Ascending	20200609	Ascending
20200621	Ascending	20200703	Ascending
20200715	Ascending	20200727	Ascending
20200808	Ascending	20200820	Ascending
20200901	Ascending	20200913	Ascending
20200925	Ascending	20201007	Ascending
20201019	Ascending	20201031	Ascending
20201112	Ascending	20201124	Ascending
20201206	Ascending	20201218	Ascending
20201230	Ascending	20210111	Ascending
20210123	Ascending	20210204	Ascending
20210216	Ascending	20210228	Ascending
20210312	Ascending	20210324	Ascending
20210405	Ascending	20210417	Ascending
20210429	Ascending	20210511	Ascending
20210523	Ascending	20210604	Ascending
20210616	Ascending	20210628	Ascending
20210710	Ascending	20210722	Ascending
20210803	Ascending	20210815	Ascending
20210827	Ascending	20210908	Ascending
20210920	Ascending	20211002	Ascending
20211014	Ascending	20211026	Ascending
20211107	Ascending	20211119	Ascending
20211201	Ascending	20211213	Ascending
20220106	Ascending	20220118	Ascending
20220130	Ascending	20220211	Ascending
20220223	Ascending	20220307	Ascending
20220319	Ascending	20220331	Ascending
20220412	Ascending	20220424	Ascending
20220506	Ascending	20220518	Ascending
20220530	Ascending	20220611	Ascending
20220623	Ascending	20220705	Ascending
20220717	Ascending	20220729	Ascending
20220810	Ascending	20220822	Ascending
20220903	Ascending	20220915	Ascending
20220927	Ascending	20221009	Ascending

Table 1 Sentinel-1 Ascending Track Image Data Adopted in this Paper

Date	Track Direction	Date	Track Direction
20200128	Descending	20200209	Descending
20200221	Descending	20200304	Descending
20200316	Descending	20200702	Descending
20200714	Descending	20200726	Descending
20200807	Descending	20200819	Descending
20200831	Descending	20200912	Descending
20200924	Descending	20201006	Descending
20201030	Descending	20201111	Descending
20201123	Descending	20201229	Descending
20210110	Descending	20210122	Descending
20210615	Descending	20210627	Descending
20210709	Descending	20210721	Descending
20210802	Descending	20210826	Descending
20210907	Descending	20210919	Descending
20211013	Descending	20211025	Descending
20211106	Descending	20211118	Descending

Table 2 Sentinel-1 Descending Track Image Data Adopted in this Paper

In this paper, the precise orbit ephemerides (POD) of Sentinel-1 satellite was used for orbital error correction; an external digital elevation model (DEM) with data resolution of 30m was adopted to remove terrain effects, of which the absolute elevation accuracy meets the DEM accuracy required by

Sentinel-1 medium resolution data. This lays a good foundation for deformation calculation.

3. RESARCHMETHOD

3.1 Short Baseline Interferometry Measurement

Considering the complex terrains in western Beijing, SBAS-InSAR technology was adopted for deformation information extraction. This technology performs better in identifying fast deformation by controlling temporal and perpendicular baseline thresholds, which is able to prevent temporal de-coherence caused by fast deformation. The algorithm principle of monitoring ground subsidence with this method mainly involves interferogram generation, stable point target extraction, Delaunay triangulation network-based estimation of linear deformation rate and elevation error, and estimation of nonlinear deformation quantity. The flow chart of SBAS-InSAR technology is as shown in Figure 3.

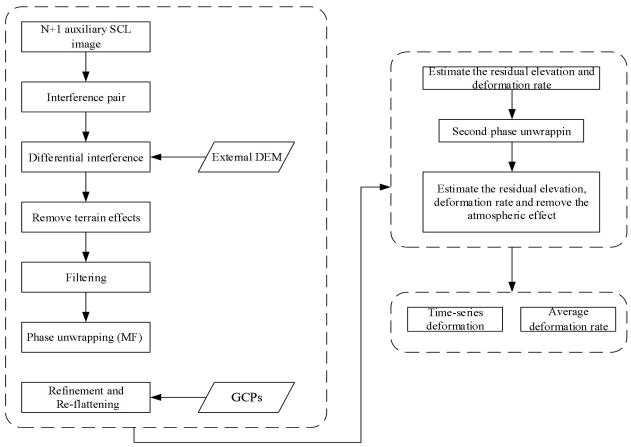

Figure 3. SBAS-InSAR data processing process

3.2 Interference Processing

For this research, GMTSAR software was employed for registration, interferometry, coherence calculation, topographic phase removal and filtering of SAR data, and then SNAPHU software was used for phase unwrapping of the interferograms. The interferogram of January 5, 2020 was selected as the main image, and that of January 17, 2020 as the auxiliary image. The comparison of interferograms before and after unwrapping is as shown in Figure 4. The left interferogram is before unwrapping, and the right one is after unwrapping.

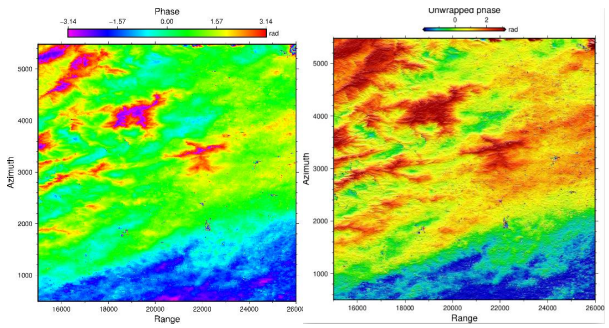

Figure 4 Interferograms Before and After Wrapping

Select the Sentinel-1B interferometric wide image of any scene as the super main image, register the rest images with the super main image, and set the temporal baseline threshold (TBT) and perpendicular baseline threshold (PBT). N+1 SAR images can generate at most M differential interferograms, and satisfy the following relational equations:

$$(N+1)/2 \leqslant M \leqslant N((N+1)/2)$$

Analyze the temporal baseline and perpendicular baseline distance of SAR images, and set the maximum temporal interval baseline threshold as 36d and the perpendicular baseline threshold as 149m. Generate interferograms corresponding to the main and auxiliary images based on the combination list of small baseline pairs, namely conducting complex conjugate multiplication of the two images and removing flat-earth and topographic phase.

3.3 Deformation Quantity Inversion

Obtain deformation results in terms of time series by calculating linear deformation rate and nonlinear deformation phase based on residual phase separation nonlinear deformation phase and atmospheric effect phase, and then conduct parameter calculation, linear deformation rate calibration, accumulative deformation quantity calculation, etc.

4. INTERPRETATION OF RESULT

4.1 Deformation Analysis of Whole Pipeline by Time Period

Comparative analysis was made on the results of the ascending track data processing by time period, and a graph reflecting surface deformation rates of western Beijing for the periods of 2020/1-2022/5, 2020/1-2022/6, 2020/1-2022/8 and 2020/1-2022/10 was developed (Figure 5). In the period of 2020/1-2022/5, the surface deformation rate in the area along the pipeline was -60 mm/year ～ 23 mm/year; in the period of 2020/1-2022/6, the surface deformation rate in the area along the pipeline was -55 mm/year ～ 20 mm/year; in the period of 2020/1-2022/8, the surface deformation rate in the area along the pipeline was -48 mm/year ～ 28 mm/year; in the period of 2020/1-2022/10, the surface deformation rate in the area along the pipeline was -43 mm/year ～ 25 mm/year. As shown in the figure, the main urban area of western Beijing was in stable condition, and subsidence occurred in an area of northwestern Haidian District.

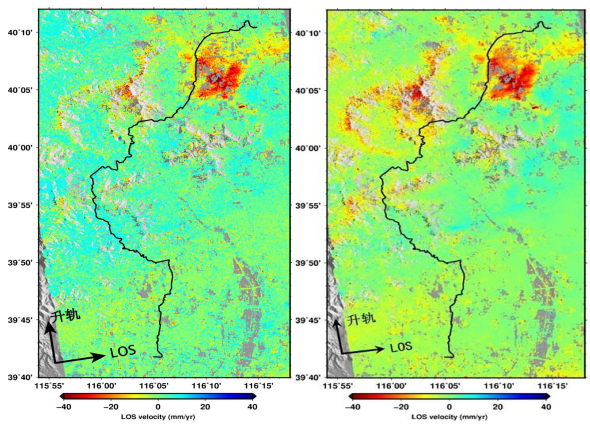

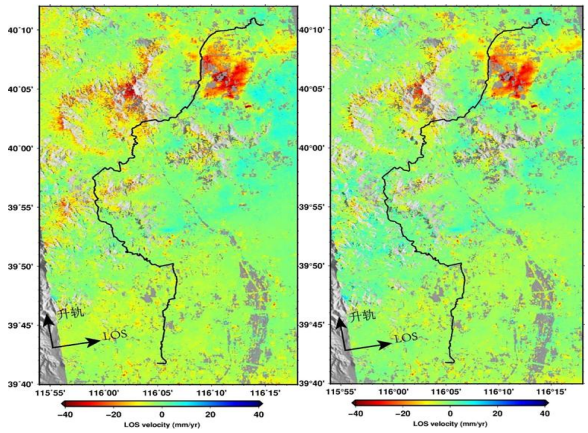

Figure 5 Surface Deformation Rate of Research Area (Ascending track data of the four periods in order: 2020/1-2022/5, 2020/1-2022/6, 2020/1-2022/8 and 2020/1-2022/10).

Surface deformation rate of the area within 1km away from the pipeline (as shown in Figure 6) was extracted, and deformation rate data of the area within 1km away from the pipeline was selected. SRTM DEM of resolution 30m was selected as the background. It is shown that surface deformation occurred along the pipeline at different degrees, and the sedimentation rate ranges in the four periods are -36 mm/year～22 mm/year, -39 mm/year～15 mm/year, -41 mm/year～15 mm/year and -39 mm/year～16 mm/year respectively. Terrains and geographical realities should be considered to further determine whether there exists any hidden geological hazard like unstable slope, surface subsidence or landslide and decide the potential risk the pipeline is faced in combination with actual conditions.

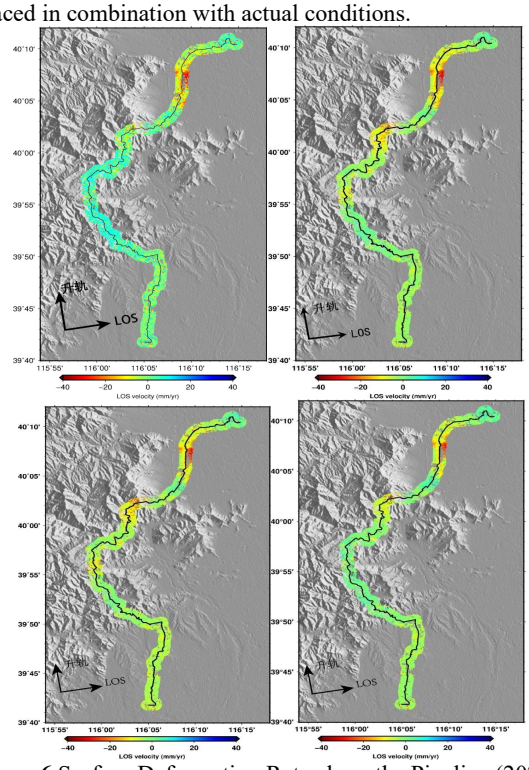

Figure 6 Surface Deformation Rate along the Pipeline (2020/1-2022/5, 2020/1-2022/6, 2020/1-2022/8 and 2020/1-2022/10).

4.2 Analysis of Fast Deformation Period and Area

Based on analysis of processing results of fast deformation period and area data, a graph (Figure 7) was developed to reflect surface deformation rates of western Beijing since January of 2020 until December 2021. The annual average deformation rate of the research area of the ascending track data ranges from -69 mm/year to 40 mm/year, and that of the descending track data ranges from -67 mm/year to 46 mm/year. The solid black line indicates the position of pipeline, and P1 and P2 are locations where cumulative deformation points were extracted.

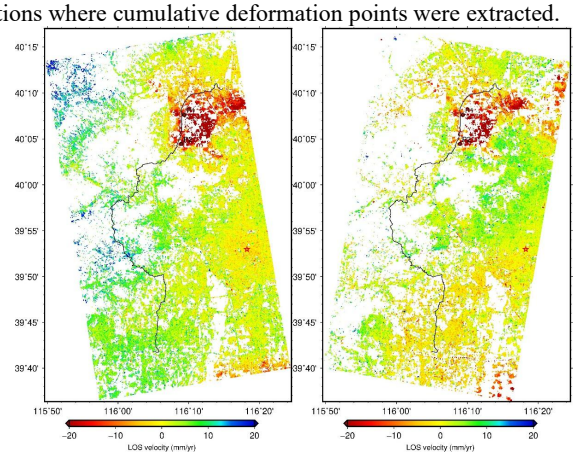

Figure 7 Surface Deformation Rate in Radar Line-of-Sight (LOS) of Period 2020/1-2021/12. Left: Ascending track; Right: Descending track.

Surface deformation rate of the area within 1km away from the pipeline (as shown in Figure 8 (Left: ascending track; right: descending track)) was extracted, and deformation rate data of the area within 1km away from the pipeline was selected. SRTM DEM of resolution 30m was selected as the background. It is shown that surface deformation occurred along the pipeline at different degrees, at the rate ranging from -44 mm/year to 34 mm/year in the ascending track, and ranging from -54 mm/year to 46 mm/year in the descending track.

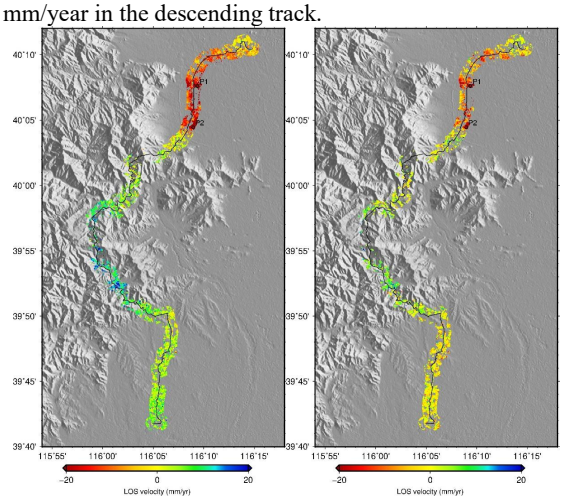

Figure 8 Surface Deformation Rate in Radar Line-of-Sight (LOS) along the Pipeline of Period 2020/1-2021/12

Two points (P1, P2) in the area where the deformation rate was large shown in Figure 8 were selected for extracting deformation time series, and Figure 9 was developed on this basis. Black points indicate ascending track data, and red points indicate descending track data. According to the figure, heavy subsidence occurred around P1 and P2, and the trend directions of the ascending track data and descending track data are highly consistent. This shows a large quantity of deformation occurred at P1 and P2 since January of 2020 until December of 2021, with the maximum deformation quantity of -70mm at P1, and the maximum deformation quantity of -50mm at P2. This result

provides a reliable reference for safety monitoring and repair & maintenance of the pipeline.

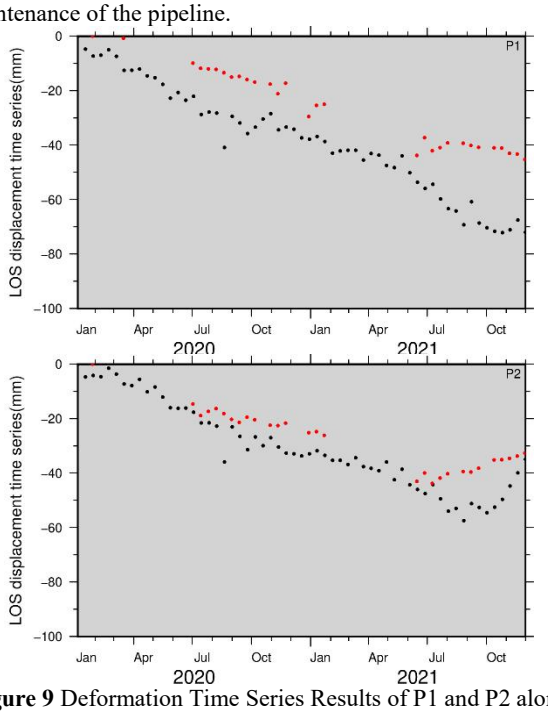

Figure 9 Deformation Time Series Results of P1 and P2 along the Pipeline

5. CONCLUSION

In this paper, surface deformation information of Beijing from January 2020 to October 2022 was extracted through time-series interferometric processing of Sentinel-1 ascending track data of 84 scenes and Sentinel-1 descending track data of 33 scenes by virtue of SBAS-InSAR technology, and the annual average deformation rate turned out to be -43mm/year ～ 25mm/year. Meanwhile, the current surface deformation status along the pipeline was extracted, and the result shows that surface deformation occurred along the pipeline at different degrees. Comparative analysis of results of the ascending track data processing shows that the surface deformation rate of the area within 1km away from the pipeline in the period 2020/1-2021/12 ranges from -40 mm/year to 13 mm/year, that in the period 2020/1-2022/5 ranges from -36 mm/year to 22 mm/year, that in the period 2020/1-2022/6 ranges from -39 mm/year to 15 mm/year, that in the period 2020/1-2022/8 ranges from -41 mm/year to 15 mm/year, and that in the period 2020/1-2022/10 ranges from -39 mm/year to 16 mm/year. The possible causes of the deformations mainly include surface subsidence, groundwater mining and such factors. Precautionary measures need to be enhanced for the area at potential risk of surface subsidence, to get rid of the threat of sudden geological disasters and resulting losses particularly in extreme weather conditions. At the same time, terrains and geographical realities should be considered to further determine whether there exists any hidden geological hazard like unstable slope, surface subsidence or landslide and decide the potential risk the pipeline is faced in combination with actual conditions.

ACKNOWLEDGEMENTS

This work was supported by National Key R&D Program Major Natural Disaster Prevention and Control and Public Safety Key Special Funding (No.2021YFC3000503).

REFERENCES

XIAO Weifeng, YANG Wentao, LI Chaokui, et al., 2020. Detection of Influence Factors and Their Interaction of Land Subsidence in Beijing Based on PS-InSAR. Geomatics World 27(06), 7-13.

JIA Sanman, Tian Fang, Qi Qian, 2019. Urban "chronic diseases"-the cause of land subsidence and comprehensive prevention and control measures. City and Disaster Reduction (3), 22-27.

GAO Ertao, FAN Donglin, FU Bolin et al., 2019. Land Subsidence Monitoring of Nanjing Area Based on PS-InSAR and SBAS Technology. jgg 39(2), 158-163.

Wang Xiaoqing, Zhang Peng, et al., 2018. Mitigation Atmospheric Effects in Interferogram With Using Integrated MERIS/MODIS Data and A Case Study Over Southern California. The International Archives of the Photogrammetry, Remote Sensing and Spatial Information Sciences, Volume XLII-3.

Rizzoli P, Martone M, Gonzalez C, Wecklich C, Borla Tridon D, Bräutigam B, et al., 2017. Generation and performance assessment of the global TanDEM-X digital elevation model. ISPRS J Photogramm Remote Sens, 132, 119–39.

HU C, Li Y, Dong X, Wang R, Cui C., 2017. Optimal 3D deformation measuring in inclined geosynchronous orbit SAR differential interferometry. Sci China Inf Sci, 60(6), 06-13.

Zheng W, Hu J, Zhang W, Yang C, Li Z, Zhu J, 2017. Potential of geosynchronous SAR interferometric measurements in estimating three-dimensional surface displacements. Sci China Inf Sci,60(6), 64-72.

Hu C, Li Y, Dong X, Wang R, Cui C, Zhang B, 2017. Three-dimensional deformation retrieval in geosynchronous SAR by multiple-aperture interferometry processing: theory and performance analysis. IEEE Trans Geosci Remote Sensing , 55(11), 61–69.

X. Lv,B. Yazıcı,M. Zeghal,et al., 2014. Joint-scatterer processing for time-series InSAR. IEEE Transactions on Geoscience and Remote Sensing, 52(11), 7205-7221.

Wang Q Q,Huang Q H,He N,et al, 2020. Displacement monitoring of upper Atbara dam based on time series InSAR. Survey Review, 52(375), 485-496.

D. Perissin,C. Prati,F. Rocca,et al., 2009. PS-InSAR analysis over the Three Gorges Dam and urban areas in China. Urban Remote Sensing Joint Event, 2009, 1-5.

Yang Q, Ke Y, Zhang D, et al., 2018. Multi-scale analysis of the relationship between land subsidence and buildings: A case study in an eastern Beijing Urban Area using the PS-InSAR technique. Remote Sensing, 10(7), 1006-1008.

Solari L, Ciampalini A, Raspini F, et al., 2016. PS-InSAR analysis in the Pisa urban area (Italy): A case study of subsidence related to stratigraphical factors and urbanization. Remote Sensing, 8(2), 120-128.

Zhu L, Gong H, Li X, et al., 2015, Land subsidence due to groundwater withdrawal in the northern Beijing plain. Engineering Geology, 193, 243-255.

WANG Xiaoqing, DANG Ya-min, ZHANG Peng, et a1., 2012. Application of MERIS atmospheric water vapor to ASAR interferogram correction. Progress in Geophysics, 27(6), 2335-2341.

ZHANG Ling, GE Daqing, GUO Xiaofang, et.al., 2014. Land Subsidence in Cangzhou over the last Decade Based on Interferometric Time Series Snalusis. Shanghai Land and Resources, 35(4), 72-75,80.